Received: 9 February 2023 | Revised: 22 March 2023 | Accepted: 22 March 2023

DOI: 10.1002/app.53961

RESEARCH ARTICLE

Applied Polymer SCIENCE WILEY

Failure analysis of fiberglass cover used for photovoltaic plants

Francesco Cepolina[1] | **Serena Gabrielli**[2] | **Guido Ferla**[2] | **Enrico Marcantoni**[2] | **Lorenzo Spinelli**[3]

[1]Department of Mechanical Engineering, DIME, University of Genoa, Genoa, Italy

[2]Department of Organic Chemistry, University of Camerino, Camerino, Italy

[3]Chemical Department, Elantas Europe S. r.l., Ascoli Piceno, Italy

Correspondence
Francesco Cepolina, Department of Mechanical Engineering, DIME, University of Genoa, Genoa 16145, Italy.
Email: francesco.cepolina@edu.unige.it

Abstract

Cover boxes with inspection glass are generally used outdoors for photovoltaic systems. Sometimes these boxes break, during normal use. High temperature, thermal stress, cyclic stress, and cracking contribute to weakening the polymeric inspection "glass". The study presents an interdisciplinary analysis to discover the mode of occurrence and causes of the failure. First, the material is accurately characterized. Then its mechanical behavior is characterized in a virtual scenario that reconstructs the real external environment. The goal is to build a new cover with inspection boxes that exhibits superior life cycle behavior when exposed to harsh weather conditions and atmospheric agents. The breaking phenomena of solar panels covering boxes in PMMA (Poly Methyl Methacrylate) are examined. Environmental stress is the main responsible for cracking. Styrene is employed in the polymerization process of Sheet Molding Compound (SMC); the diffusion of this material is the main responsible for cracking. Comprehensive engineering analysis shows how the thermoplastic component fails after being exposed to atmospheric agents. The PMMA "glass" is one of the polymers most sensible to the crazing phenomena.

KEYWORDS

environmental stress crazing, PMMA crazing, PMMA laboratory tests, product optimization, styrene influence on PMMA

1 | INTRODUCTION

The quest for materials used in the creation of new products is growing quickly today. It is important to pay close attention to studying the characteristics and behavior of materials.[1–3] Growing environmental awareness requires considering the entire material life cycle, including reuse, and recycling. Depending on the working environment and the operations carried out, the mechanical qualities of materials might degrade, clearly harming both suppliers, and users.

Aggressive environmental agents[4] may form cracks in polymers. The stress, breaking the small fibrils on the edges of these cracks, can cause structural failure.[5,6] In recent decades, extensive research on these phenomena have been performed.[7,8] The material properties are influenced by biological organisms, water, solvents, sunlight, oxygen, heat, ozone, ionizing radiation, and volatile organic compounds.[1–3] There are, however, still few investigations on the outcomes of the interactions between structural stresses and environmental

influences; this research aims to give an original contribution to these aspects.

Styrene is a volatile organic agent that penetrates glassy polymers and facilitates the formation of cracks in PMMA. Styrene contributes to the crazing phenomena.[9,10] The issue being addressed is interdisciplinary and complex. Due to the large number of variables involved, the answer cannot be tackled solely theoretically. Moreover, the behavior of the phenomena studied is nonlinear. Therefore, an experimental method has been used; a systematic test campaign has been adopted to characterize the materials.

The mechanical behavior of the reference components has been investigated using Creo, a solid modeling software from PTC. Structural and dynamic analyses have been simulated in different environmental scenarios.

Section 2 introduces a box for solar panels and the production technologies of the polymeric material.

Section 3 describes a wide range of laboratory tests performed on samples of PMMA.

Section 4 describes the characterization of the PMMA material; the mechanical properties of the material depend on the temperature.

Section 5 is devoted to structural analyses in a virtual environment, under different loads and disturbances.

Section 6 describes some outdoor climatic and vibrational tests.

Section 7 reports the conclusions along with some suggestions for potential future developments.

2 | REFERENCE PRODUCT AND PRODUCTION TECHNOLOGY

The reference product is an electric cabinet with a closing door made of PMMA rather than glass. The transparency of this material enables visual inspection of the electrical parts inside the cabinet.

Due to its mechanical strength—high Young's modulus and low elongation at the break—PMMA is light. Low humidity absorption ensures good dimensional stability.[11] The resistance to chemicals and atmospheric agents is excellent.

The cover frame is made of Thermoset SMC: a blend of polymer resin, inert fillers, fiber reinforcement, catalysts, pigments, and stabilizers. SMC has excellent dielectric properties.

Plate molding compounds are produced by casting a layer of thermosetting resin onto a carrier sheet of polymeric film. The resin is an unsaturated polyester composition containing monomer styrene, chopped fiberglass, and filler.

Before molding, the viscosity of the resin paste is increased. SMC is a "putty-like" material that drifts the fibers during compression molding. The sheets can be easily handled.[12,13]

The molding is a critical phase: the styrene, responsible for hardening, is present in a very high concentration. Not all monomer is polymerized. The residue's volatile styrene monomer can migrate into another material, such as PMMA.[14]

3 | EXPERIMENTAL TESTS

The transparent thermoplastic PMMA, employed in the experiment, has a tensile strength of 45 MPa and an elastic modulus of 1900 N/m^2. The material has a density of 1.19 g/cm^3, a flexural strength of 79 MPa, and an impact resistance-Izod of 5 KJ/m.

The SMC employed is a fire-retardant grade, halogen-free, and glass fiber-reinforced sheet molding compound based on an unsaturated polyester resin. This SMC, developed for electrical applications, has a density of 1.65 g/cm^3, a flexural strength of 140 MPa and an impact strength (Charpy) of 65 KJ/m^2.

PMMA plate samples have been sliced using a razor blade (10 × 10 mm). Three types of samples have been prepared: used PMMA plates subjected to rupture, used PMMA not subjected to rupture and new standard PMMA. The samples have been analyzed to check for any differences among them.

The amount of styrene has been measured. The mechanical properties of materials can degrade due to several factors such as crazing, polymer degradation, physical aging, or chemical reactions. We have performed the following analyses to confirm that PMMA was degraded only due to crazing: Fourier Transform Infra-Red attenuated total reflection (FTIR-ATR), spectroscopy, Electron Scanning Microscopy (SEM), and headspace-Solid Phase Micro-Extraction (HS-SPME) coupled with gas chromatography–mass spectroscopy (GC–MS).

3.1 | Infrared spectroscopy

A promising technique for examining any chemical alteration of the polymer is FTIR-ATR spectroscopy, which quantifies the movement of small molecules within polymers. This technique has increasingly been used to study sorption kinetics in polymers and has proven to be very accurate and reliable. The distance from the interface, which is on the order of micrometers, makes ATR generally insensitive to sample thickness, allowing for dynamic measurement in a layer with a certain thickness.[15]

By increasing the refractive index of the ATR crystal, the depth of penetration will decrease (i.e., changing from ZnSe to Ge, with refractive indices equal to 2.4 and 4, respectively). This will decrease the effective path

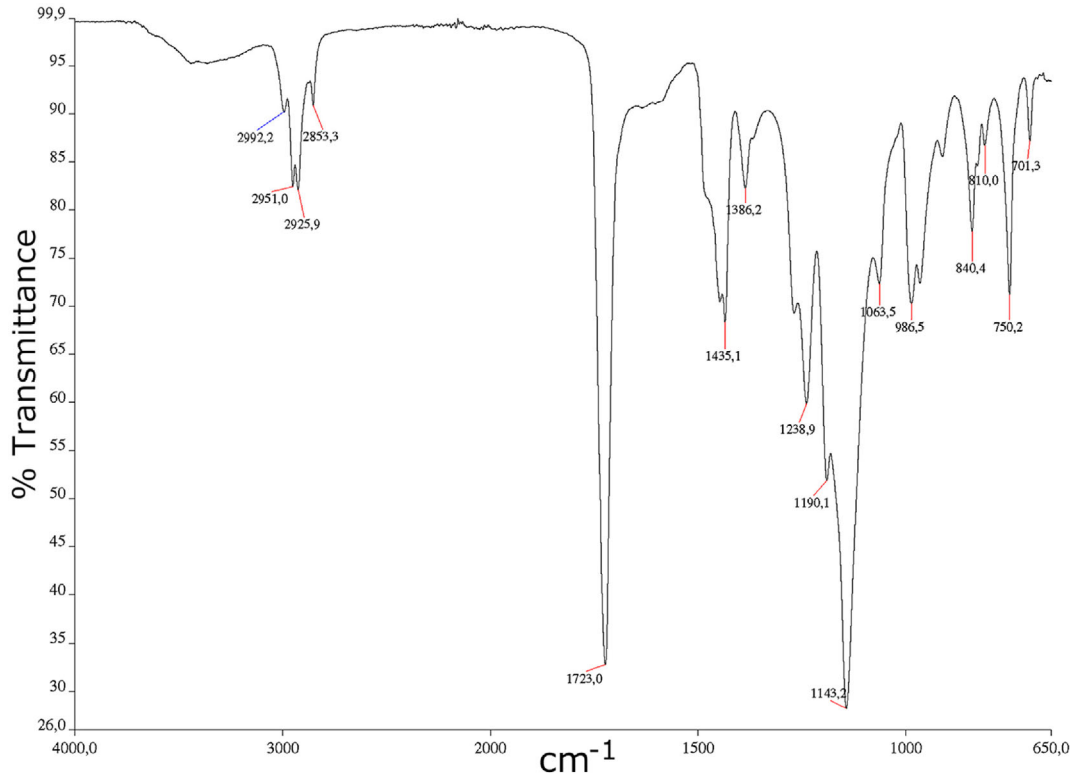

FIGURE 1 The FTIR spectrum of PMMA without any fracture. [Color figure can be viewed at wileyonlinelibrary.com]

length and, therefore, decrease the absorbance intensity of the spectrum. Infrared spectroscopy has been used to characterize the chain structure of polymers and has led the way in interpreting the mechanism to ensure any chemical degradation of the PMMA plate.

The study of the spectrum has shown that no chemical degradation has occurred. There has been no evidence of chemical degradation of PMMA. These results support the physical mechanism that occurred in the PMMA plate under test.[16] The FTIR spectrum in Figures 1 and 2 displays two distinct bands at 2923 and 2853 cm^{-1} that, respectively, correspond to the asymmetrical and symmetrical CH_3 stretching vibrations of PMMA. These absorption lines were identified as typical infrared bands of PMMA. Frequency 1723 cm^{-1} is assigned to the C═O stretching vibration. Bands at 1435 and 1386 cm^{-1} correspond to asymmetrical and symmetrical CH_3 bending vibrations, respectively. The C—O (ester bond) stretching vibration is represented by wider and stronger bands in the region of 1000–1300 cm^{-1}. C—H bending out-of-plane is attributed to the peak at 750 cm^{-1}.

The FTIR spectroscopy measurements in the 400–4000 cm^{-1} range were performed on a Perkin-Elmer spectrometer "Frontier". The multiple internal reflectances (MIR) technique with a GeSe crystal has been used. The spectra were gathered using 16 scans at a resolution of 2 cm^{-1}, and a Perkin-Elmer data manager (Spectrum) was used to analyze them.

3.2 | Electron microscopy

The surface morphology of polymers is frequently studied via scanning electron microscopy (SEM). The method employs a main electron beam that interacts with the specimen of interest in a vacuum environment to produce a variety of electron types and electromagnetic waves. The secondary electrons emitted from the specimen surface are collected and displayed to provide a high-resolution micrograph.[17–19]

Nonconductive specimens, such as organic compounds, which tend to charge when scanned by the electron beam, especially in the secondary electron imaging mode, require careful consideration. Due to this, image artifacts and scanning errors are generated. To protect them, they are typically coated with an extremely thin layer of an electrically conductive material, typically gold, which is deposited on the sample using either a low vacuum sputtering machine or a high vacuum evaporation unit. In this investigation, SEM (LEO 1450 VP-SEM, variable pressure) was used to characterize the morphology of the PMMA plates at accelerating voltages ranging from 0.2 to 30 kV. To improve imaging, a 20 nm film of gold was applied to all samples before the observation (Agar coating unit PS3). The first step was to employ SEM analysis to identify what caused the rupture of the PMMA polymer composites' cross-sectional area. We

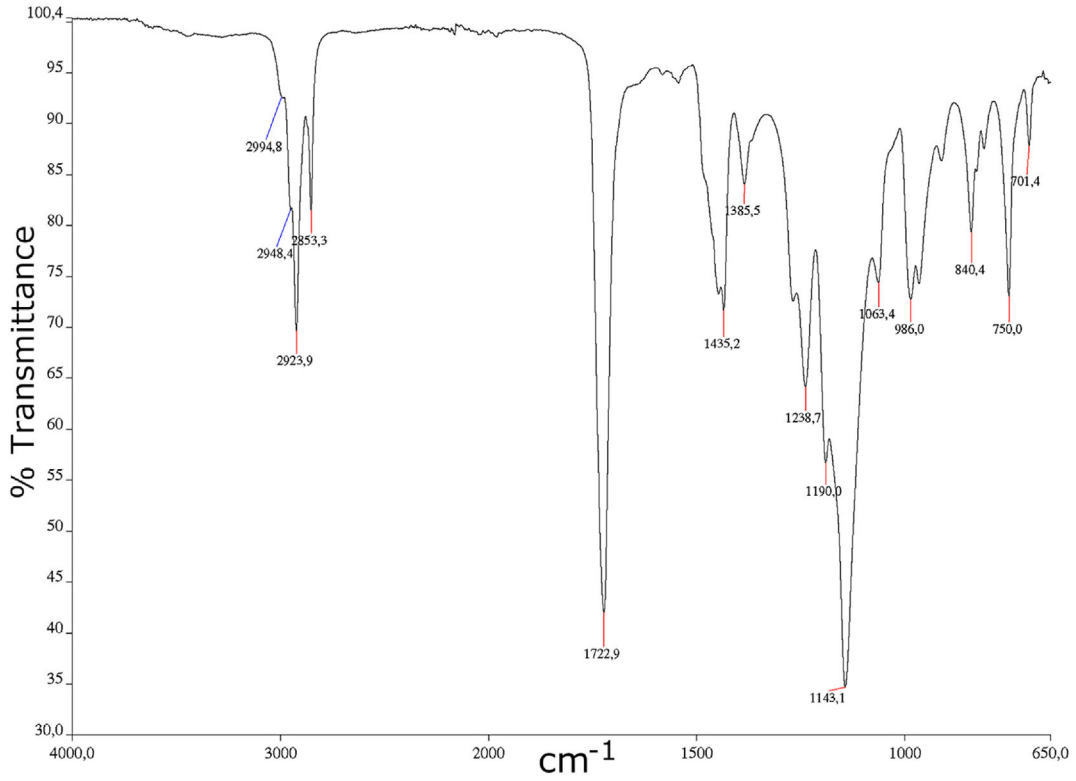

FIGURE 2 The FTIR spectrum of PMMA with fracture. [Color figure can be viewed at wileyonlinelibrary.com]

hypothesized, based on the spectrum, that the failure was caused by the normal behavior of most polymer composites. When the PMMA composite's inorganic filler is exposed to extreme temperature fluctuations (in-service environment), the thermal stress increases and leads to failure due to cracking.[20] In a polymeric organic matrix, the inorganic particles typically tend to aggregate. Once the agglomeration is large enough, the terminal link in the polymeric chain may break or the particle may crack. The organic component of the polymeric mix may undergo chemical breakdown in either situation.

Imaging by SEM our samples revealed a contrasting band running through the panel. Backscatter image mode produced significant Z-contrast: the band contains inorganic elements. The presence of many fibrils indicates the craze formation and the next crack generation (Figure 3).

3.3 | Head space-solid phase microextraction coupled with gas chromatography mass spectroscopy

Thanks to SPME technology, volatile substances with a wide range of boiling points can be analyzed without the creation of artifacts.[21,22] In SPME, volatile compounds are extracted from the headspace of solid or liquid samples and placed on a fused-silica fiber coated with a polymeric phase.[23]

All the analyses were conducted on Agilent 5973 inert GC/MS system, with an EI system electron source. This method has been employed for the analysis of PMMA-SMC front doors (Supelco, Bellefonte, PA). 2.0 g of PMMA plate was first ground, and 1.0 g of the ground sample was then weighed into 4.0 mL SPME flasks complete with screw-top covers and PTFE/silicone septa. The following SPME fibers (Supelco, Bellefonte, PA) were tested in this study: gray 50/30 μm divinylbenzene carboxen polydimethylsiloxane (DVB/CAR/PDMS), and red 100 μm polydimethylsiloxane (PDMS).

According to the manufacturer's instructions, these fibers were conditioned before use, respectively at 270°C for 1 h and 250°C for 30 min. These fibers were tested to determine which one has the best ability to extract the composite volatiles. The fibers were exposed to the sample headspace in this step under the following arbitrary conditions: equilibrium and extraction time of 30 min; equilibrium and extraction temperature of 100°C. After extraction, the fibers have been placed into the gas chromatograph injector for the desorption analyses (250°C temperature, split less mode, 3.0 min duration). The fibers were then reconditioned for 15 min at 250°C. This technique was carried out to ensure the accuracy of the SPME extraction and chromatographic processes, as well as the absence of peaks in the run blanks.

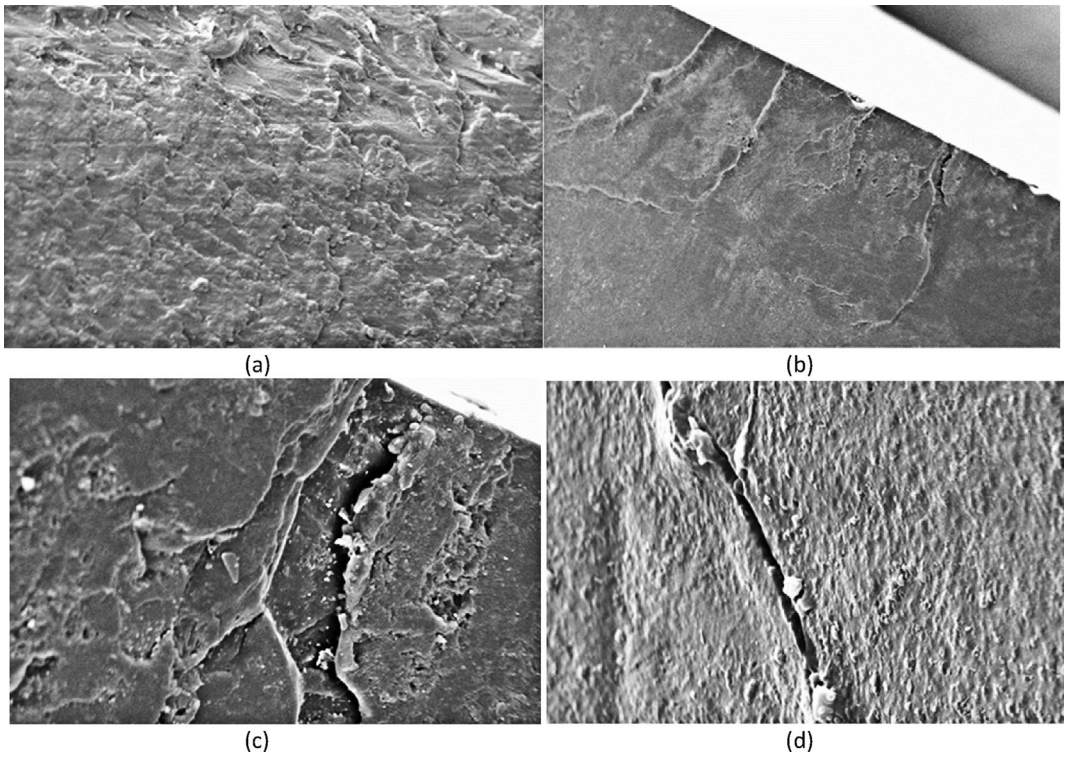

FIGURE 3 (a) SEM micrograph of new PMMA composite. Magnification: 209×. (b) SEM micrograph of crazed/cracked PMMA composite. Magnification: 65×. (c) SEM micrograph of crazed/cracked PMMA composite. Magnification: 414×. (d) SEM micrograph of crazed/cracked PMMA composite. Magnification: 3.73Kx.

The gray (DVB-CAR-PDMS) coating fiber was selected to determine the influence factors of the HS-SPME extraction efficiency of volatile compounds from PMMA/SMC plates. This SPME fiber was chosen because of its higher reproducibility in the analysis of compounds with molecular weights between 40 and 275 Da.[24,25] A high concentration of styrene can be seen in the spectrum due to the curing process used to create SMC sheets. Together with environmental factors, this high concentration explains the crazing effect that causes PMMA to fracture. This is because styrene has penetrated the polymer chains, adding a significant amount of molecular mobility to a structure where the polymer chains are typically stiff. This happens because of the low intermolecular interactions between adjacent polymer chains in comparison to the material's yield point. Molecular mobility rises together with the local free volume in the region of these chains. Cavitations consequently occur inside this softened material. In the presence of a crazing agent, these intermolecular forces tend to weaken even more, which causes the shrinkage of the surface layer and the formation of cracks.[26]

The presence of surface cracks can increase the extent of degradation by providing a pathway for styrene to penetrate deeper into the sample. The observed cracking on the surface shows the loss of mechanical properties of PMMA "glass" doors. The SEM has shown that, before cracking, the mechanical properties have decreased considerably. Most likely, micro-cracks not detectable by SEM, also contribute to the loss of mechanical properties.[27] The mechanical characteristics of the PMMA "glass" can degrade because of this phenomenon, caused by the presence of chemical compounds like styrene. "Environmental crazing" is a physical phenomenon that causes microcracks to occur by producing a local yield and plasticizing the area that has been under the highest stress. The micro-cracking can lead to a breakage of the material surface, without changing the chemical nature of the organic component. The experimental tests reported in this study confirm that the environmental stress-crazing phenomena[28] are the main cause of the crack formation in PMMA "glass" doors on SMC.

4 | MATERIAL CHARACTERIZATION

Temperature-related changes in material properties are significant. The commercial PMMA used has a traction strength of about 45 MPa at 20°C. The same material has a traction strength of 25 MPa at 60°C; 20 MPa of resistance is lost due to the 40°C temperature rise.

For more accurate results some PMMA performance/temperature curves have been searched in the literature.[29]

Photovoltaic plants can be installed in different places. The peak temperature can be recorded in the summertime, mid-day, on the sea level. The lowest temperature is reached during the winter, at night on the mountain. The temperature range considered for a photovoltaic plant (−20/+60°C) is used as a target temperature. In fact, cycle 1 (Figure 12) was performed with temperature cycles equal to T_{min} −20°C and T_{max} +65°C.

The temperature range considered is from −20 to +60°C. These graphs have been studied and interpolated to know the behavior of the material at the target temperatures (Figure 4). It is evident from the graph that PMMA is flexible at high temperatures and fragile when cold.

The graphs of Figure 4 have been used to characterize the PMMA at the desired temperatures; the following PMMA strains have been considered (Table 1). The commercial PMMA datasheet considered,[30] has a tensile strength (ISO 527-2, R7500 = 50 MPa, R7600 = 40 MPa) 27% lower than the allowable stress reported in the literature.

The data from Table 1 have been used to create two new materials in Creo: PMMA −20°C and PMMA +60°C. A separate thermal analysis has been done for each of the two temperatures.

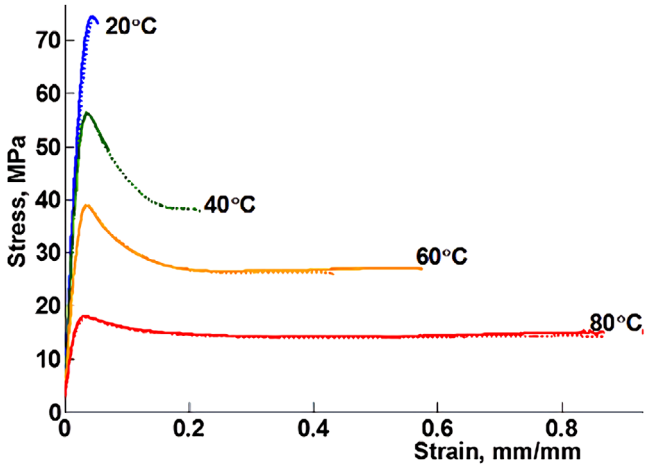

FIGURE 4 Tensile stress–strain curves of PMMA at different temperatures.[29] [Color figure can be viewed at wileyonlinelibrary.com]

TABLE 1 PMMA stress function with temperature.

Temperature (°C)	Max. allowed stress (MPa)	Declared admitted stress (−27%) (MPa)	Elastic modulus (MPa)
−20°C	85	62	7000
+20°C	60	45	1900
+60°C	23	17	500

5 | STRUCTURAL BEHAVIOR UNDER SIGNIFICANT TYPES OF LOADS INCLUDING WEATHERING

The possible loads acting on the fiberglass boxes have been evaluated. Each type of load is characterized by quantitative values. The chosen hypothesis and the calculating process are outlined below.[31]

5.1 | Accidental bumps

Virgin PMMA is an extremely impact-resistant material. We have tested the styrene contaminated PMMA in the lab to demonstrate its Izod impact resistance; the material can survive impacts up to 5 KJ/m^2. Most commercial electric boxes are certified to withstand bumps of at least 2 J; we refer to this number as a "standard bump". According to the tests performed, the PMMA polluted with according to the Izod tests has still an impact resistance much higher than the standard bump. Because of this, we believe that the contribution of accidental bumps to the break of PMMA is negligible.

5.2 | Thermal stress

The boxes for solar energy plants are typically located outside, where they are exposed to the hot sun (which is strongest in the summer), and the chilly night (coolest in winter). Temperature variations in desert regions, such as those in the Oregon region, can reach approximately 40°C. For more humid areas like Italy, the daily temperature range is often around 10°C. To be conservative, we can say that the temperature outside close to the boxes fluctuates from −20 to +45°C. It is important to know the difference in temperature between the temperature inside the box and the outside temperature, as well as the absolute temperature outside. Prudently, it is possible to say that the temperature changes by 45°C during the summer. The heat generated by the electrical equipment within the box might worsen its thermal stress since, at night and in the winter, it is warm inside the box while it is below zero degrees outside.

The fiberglass box is negatively impacted by the thermal load since it is made up of parts with various expansion coefficients. Typically, some stress is created when two objects with different thermal expansion coefficients come into contact.

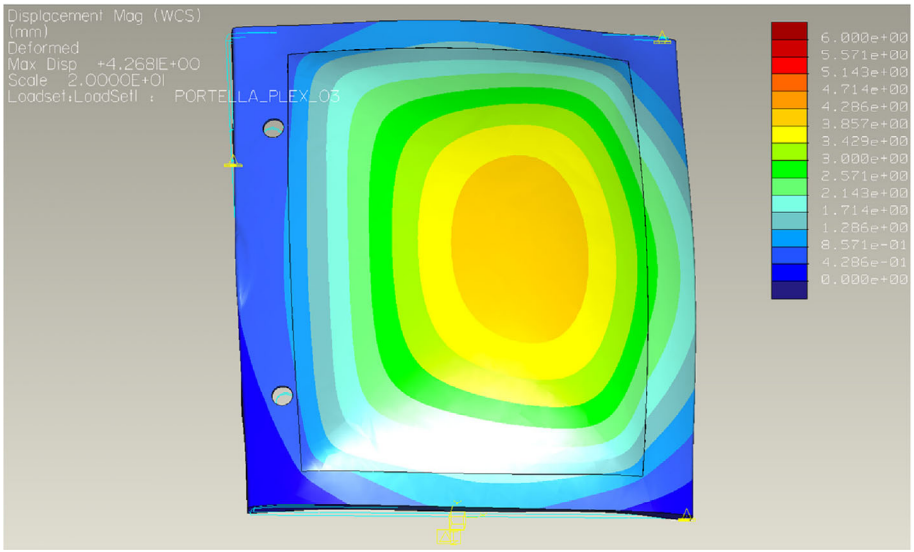

FIGURE 5 PMMA thermal stress at 45°C. [Color figure can be viewed at wileyonlinelibrary.com]

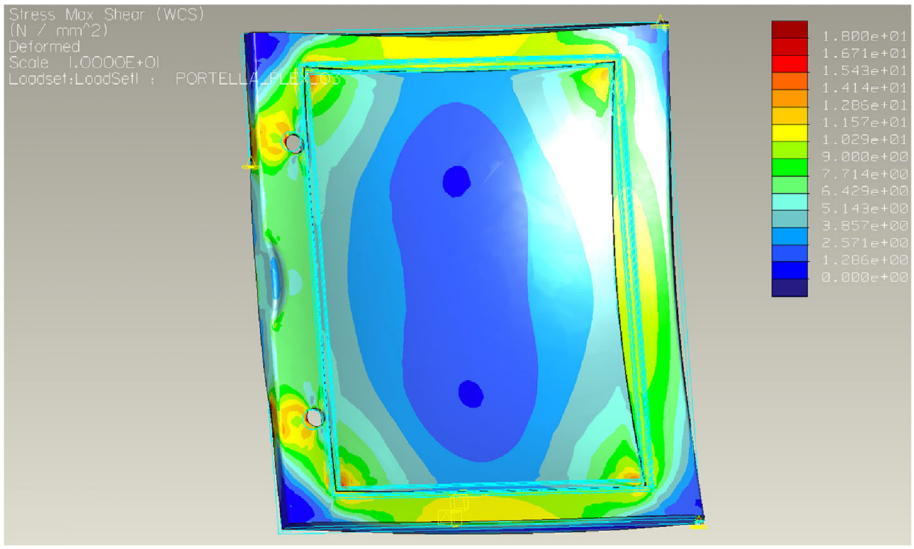

FIGURE 6 Max stress PMMA 15 MPa – PMMA thermal stress (from −20 to 45°C). [Color figure can be viewed at wileyonlinelibrary.com]

The examination of the door under thermal stress is the focus of this paragraph. Thermal, stress, and deformation simulations were carried out using PTC's commercial solid modeler Creo.[32,33] Tetrahedral elements have been used to mesh a 3D model of the box cover, and the discussed thermal loads have been applied to the model. Both the element temperature and the ambient temperature have been assigned.

Although the "glass" is welded to the door's frame, the glue holding the PMMA plate to the door is not modeled. The maximum strain on the door is 9 mm. Figure 5 shows displacements that have been increased 20 times to help comprehend the phenomenon. Figure 6 shows displacements that have also been amplified. This simulation, experimentally verified, shows how the difference in the thermal coefficients between PMMA and fiberglass tries to bend the door, putting the PMMA under stress.

The strain analysis reported in Figure 6 is interesting. The maximum "glass" stress is 10 MPa. This simulation clarifies that the single thermal strain effect is not enough to break the "glass".

5.3 | Material aging – environmental stress crazing

Acid rains can damage the boxes. As well as the wind, ice, and snow. We focused the analysis on a mechanical phenomenon, called "Environmental stress crazing". This phenomenon arises due to the presence of chemical substances that change the mechanical properties of the composite material. The PMMA under thermal stress and in presence of styrene creates a local yield and plasticizes the area most subject to stress. Consequently, micro-

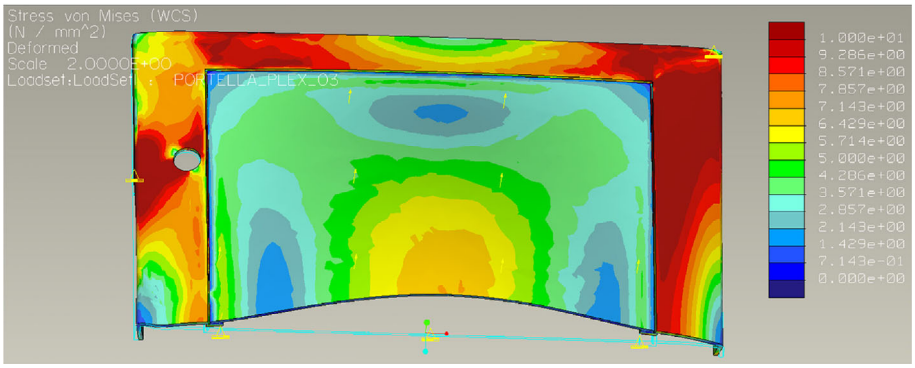

FIGURE 7 Box stress due to air expansion. [Color figure can be viewed at wileyonlinelibrary.com]

cracks are formed. The growth of these micro- cracking can lead to a breakage of the material, without changing the chemical nature of the component. An analysis of the material's chemical resistance by the Nalgene Thermo Scientific company explained that PMMA could not be in contact with styrene for longer than 30 days. In case of promulgated exposure,[34] crazing, and a lack of mechanical characteristics may occur.

The effect of material aging can be considered by assigning to it lower mechanical properties. Specific 3D modelers need to be used to simulate crack propagation. However, we can consider this effect simply assigning to the material's lower mechanical properties.

Four load tests have been performed on two pairs of specimens. All the specimens tested are in PMMA. The tests have been carried out at room temperature. The resistance section of the "butterfly" is 3×7.2 mm. The first couple of samples are in the new PMMA, and the second couple of samples are in the aged PMMA. The PMMA has been aged by plunging it for 10 min into the styrene. The new PMMA carries a load of 134 kg. The aged PMMA carries a load of 104 kg. The tensile strength of the two materials is 62 and 48 MPa respectively. This data confirms that the styrene tends to damage the PMMA. The tests have shown that the PMMA, has an admissible stress of 62 MPa; the manufacturer of the PMMA declares admissible stress of 45 MPa.

To confirm the results of the tests done, additional tests have been done on a PMMA broken door: the "butterfly" sample has a section of 7.4×2 mm; the two samples have offered a resistance of 731 N. The maximum stress is 49 MPa, this value is like the 48 MPa tested before. So, it is possible to state that the aging of the PMMA decreases its stress strength to 14 MPa (62 – 48 MPa = 14 MPa).

5.4 | Air expansion

The air, when the temperature increases, tends to increase its volume. The fiberglass box can be represented as a

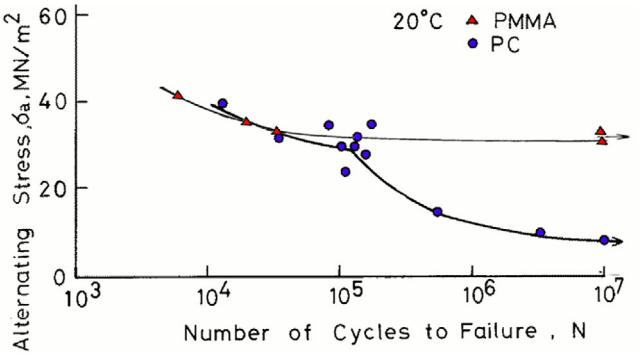

FIGURE 8 The stress of PMMA versus PC (polycarbonate) due to cyclic loads. [Color figure can be viewed at wileyonlinelibrary.com]

closed volume full of air. To describe the behavior of the air we can use the equation of the perfect gas. Assuming a temperature shift of 45°C, on the "glass" of the box is exerted a pressure of 8 N/mm^2 that leads to an overall load of 330 kg. This pressure insists on the "glass" surface. The pressure is independent of the type of material of the glass and the box. However, it is necessary to consider that the box is not completely sealed. Fiberglass boxes give IP66 protection; the seals of the box can only partially isolate the air volume inside the box.

Moreover, the electric cables, that enter the boxes, may have not airtight sealing. It is difficult to know exactly the level of tightness of the seal, we can assume that 1/10 of the found force (33 kg), is exerted on the "glass" of the door. This pressure, alone, creates a "glass" stress of 7 MPa (Figure 7). This simulation only considers the load due to the air pressure and does not include, for example, the strain of the materials due to the different dilatation coefficients.

5.5 | Cyclic loads

It is important also to evaluate the cyclical nature of the loads.[35] Specifically, the effects of the temperature on the

box, which are reflected in the expansion of the material and on the air pressure, are applied with a cyclic frequency. In the case of PMMA cyclic loads,[36] a specific maximum admissible stress needs to be considered (Figure 8).

If the doors statistically break 2 years after the installation, the number of night/day cycles is 2×365. The PMMA fatigue stress is considered for cycles comprised between 104 and 107 cycles. For this reason, the effect of the night/day cyclic load can be considered negligible.

Solar panels produce direct current energy. A transformer converts the DC into AC, then the electric energy enters the national power net. The transformer works at 50 Hz. The transformer is often hosted inside the boxes for solar plants. The efficiency of a transformer is about 98%, the lost energy becomes heat and vibrations. The transformer, when is on service, creates some vibrations; we assume that the created vibrations are at 50 Hz.

These cyclic vibrations may encourage the development of cracks and contribute to their propagation. The 50 Hz frequency can be considered critical. It is necessary to experimentally verify how the vibrations, generated by the transformer, are transmitted inside the box.

A body can be subject to a cyclic load; if the frequency of the load is close to the natural frequency of the body, the body can resonate. When a body resonates it gathers energy and eventually, it breaks. It is then necessary to verify the natural frequency of the box is higher than the frequency generated by the transformer. The natural frequency of the box has been evaluated thanks to the simulator Creo; the box has a natural frequency of about 1 Hz and several secondary higher frequencies; Figure 9 shows the natural frequency of the box near 50 Hz. The transformer and the box have respectively a natural frequency of 50 and 1 Hz. For this reason, while the transformer is powered, there is no risk of box resonance.

5.6 | Resistance check

The superposition principle is used to evaluate the resistance of the PMMA "glass". One or more of the loads

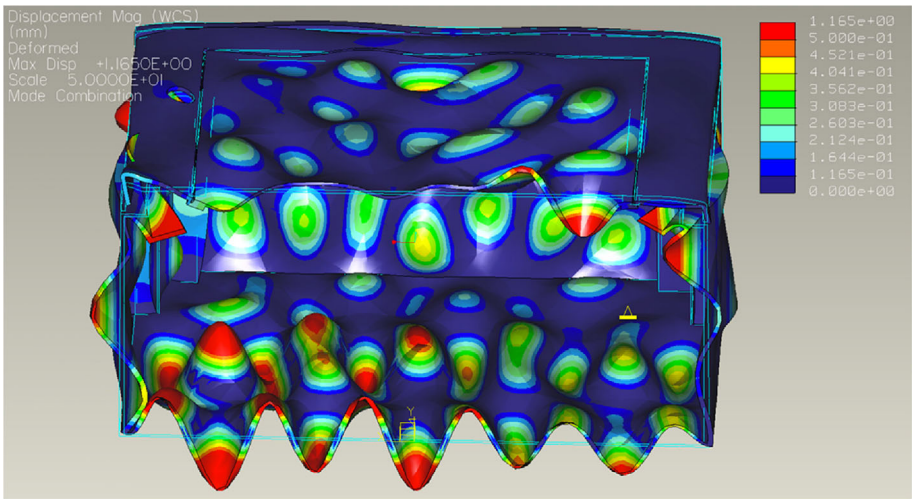

FIGURE 9 Magnified view of the box vibration. [Color figure can be viewed at wileyonlinelibrary.com]

TABLE 2 Mechanical properties of PMMA and the loads to which it is subjected.

Property/phenomena		Stress (N/mm^2)	Notes
Material	Property at −20°C	62	The cold PMMA is stiff and has an admissible stress of 62 N/mm^2.
	Property at +20°C	45	PMMA at room temperature has an admissible stress of 45 N/mm^2.
	Property at +60°C	17	At 60°C the PMMA can carry a load of 17 N/mm^2.
	Crazing	14	The PMMA becomes fragile in presence of styrene.
Loads	Accidental bumps	4	The accidental bumps load is almost negligible
	Thermal stress	Max 15	Case: glass welded on the frame, no glue and thermal stress 45°C.
		Min 2.3	Case: real glue is simulated. The thermal stress is 45°C.
	Vibrations	10	Vibrations due to the transformer load: 50 Hz load frequency.
	Air expansion	8	Thermal stress is 45°C. The seal of the box loses 90% of pressure.
	Cyclic stress	15	In the case of fatigue loads PMMA admissible stress is 30 MPa.

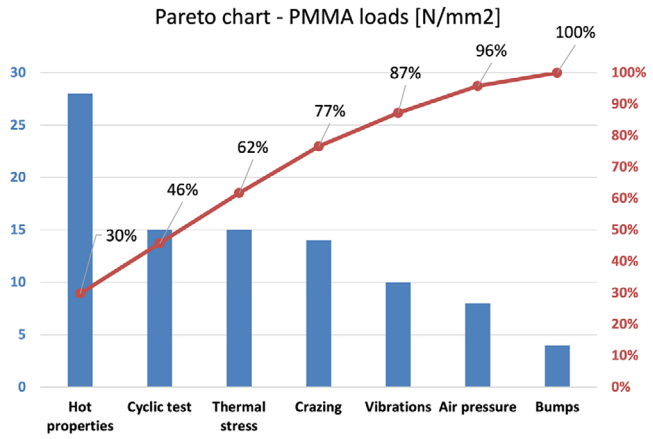

FIGURE 10 Relevance of the loads affecting the PMMA. [Color figure can be viewed at wileyonlinelibrary.com]

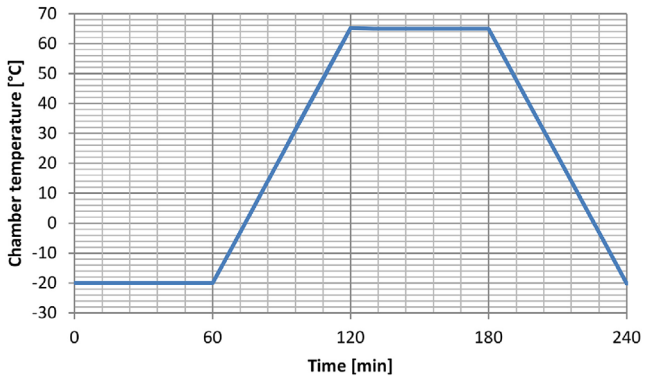

FIGURE 11 Thermal cycle 1 detail. [Color figure can be viewed at wileyonlinelibrary.com]

analyzed before can be simultaneously present. One or more of the loads analyzed in the previous paragraphs can be present at the same time. Table 2 summarizes the mechanical properties of PMMA and the loads to which it can be subjected. The percentage incidence of each phenomenon is shown in Figure 10.

6 | COMBINED CLIMATIC AND VIBRATIONAL TESTS

Some tests have been performed to recreate the stress conditions that could generate the breakage of the "glass" door. The test environment has been designed to simulate the real working conditions.[37–39] The born of cracking in the transparent thermoplastic material of the door has been reproduced thanks to chemical, temperature, and vibration tests. The styrene generates chemical stress, the temperature chamber and the environment create the thermal loads, and the transformers provide the vibrational load. The transformer thermal contribution, due to the loss of energy, is negligible as the box is not fully airtight. During the test, a powered transformer has been installed inside the box mainly to verify the vibration effect.

The same tests have been done on two samples; box #1 has a transparent "glass" door in PC and is equipped with a 2000 VA transformer, the box #2 has the PMMA "glass" door and a 500 VA transformer. The two samples have been loaded with the following chemical, vibration, and thermal stresses:

1. *cycle 1*: $T_{min} = -20°C$; $T_{max} = 65°C$; Ramp duration = 1 h; Time T_{max} = 1 h; Time T_{min} = 1 h (Figure 11);
   a. Full load operation of transformers (sources of vibrational stress)
   b. During the day recording signals from strain gage sensors
   c. Vibration recording on sample # 1 bottom
   d. Repeated cycles for 5 days
2. *cycle 2*: OUTDOOR settling period after treatment with styrene for 16 days;
   a. $T_{amb\ min}$ recorded $-4°C$; $T_{amb\ max}$ recorded $= 12°C$
3. *cycle 3*: $T_{min} = -25°C$; $T_{max} = 20°C$; Ramp duration = 1 h; Time T_{max} = 1 h; Time T_{min} = 1 h;
   a. Full load operation of the transformers (sources of vibrational stress)
   b. Repeated cycles for 8 days
4. *cycle 4*: OUTDOOR settling period after treatment with styrene for 21 days (Figure 12);
   a. $T_{amb\ min\ recorded} - 6°C$; $T_{amb\ max\ recorded} = 14°C$

During cycle 1 some strain gages have recorded the displacement of the "glass": the maximum displacement recorded (strain) is 0.2 mm on the border of the door of the sample. After this initial displacement, no additional displacement has been recorded.

During cycle 1 the vibrations induced by the operation of the 2000 VA transformer, installed, and put into operation at the rated load in sample 1 were recorded, with the following results: sinusoidal movement, frequency = 50 Hz; width = 0.5 mm (measured on the galvanized bottom of the switchboard). The vibration transmitted from the galvanized bottom to the door under test, considering an attenuation factor equal to 10 from the metal bottom to the door, should reasonably be 0.05 mm. Similar experimental tests were carried out on the samples with the described cycles. A summary of the results of the tests is here down reported (Table 3).

FIGURE 12 Cycle 4, outdoor settling time. [Color figure can be viewed at wileyonlinelibrary.com]

TABLE 3 Summary of the test results.

	Sample *n*	
Type of test	**1**	**2**
Formation of cracks in the transparent material of the door after climatic – vibrational – cycle I	No	No
Cracks in the transparent material of the door after treatment with styrene and subsequent outdoor settling – cycle 2	No	No
Formation of cracks in the transparent material of the door after climatic – vibrational – cycle 3	No	No
Cracks in the transparent material of the door after outdoor settling – cycle 4	Yes	No

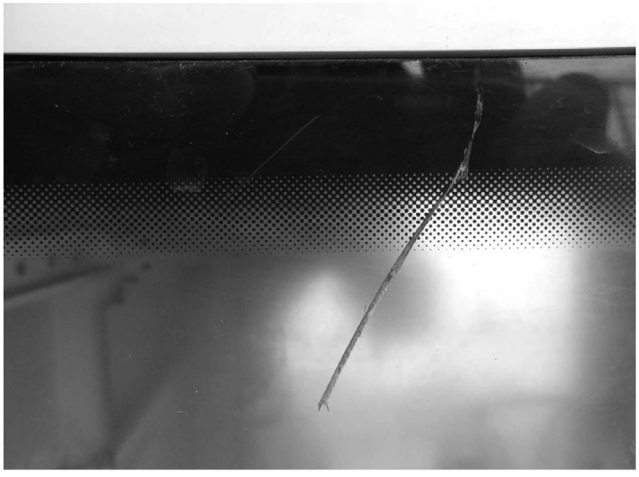

FIGURE 13 Crack propagation.

The settling time of the cycle 4 lasted 21 days (Figure 12); during this phase, cracks slowly began to appear on the edge of the PMMA window (Figure 13). The cracks have spread until they intersect each other. At the end of the tests the PMMA window broke into 4 parts while the polycarbonate porthole was intact.

The test campaigns carried out offer experimental comfort relative to the studies that have been done. Based on the results of the tests and investigations, it can be said that styrene, the primary cause of the crazing phenomena, weakens PMMA rather than PC. It was also intriguing to see that the door's breakage did not happen during the climatic chamber's cycles, but rather during the settling cycle that followed outside in the cold. This "delayed" timing is characteristic of crazing phenomena. In our case, the process was accelerated/enhanced by the further embrittlement of PMMA due to continuous exposure to low temperatures.

There is a phenomenon of fatigue breakage of the PMMA sheet due to the thermal cycles. The breakage is exclusively generated by the embrittlement of the material (PMMA), caused by the polymerization of residual styrene and low temperatures.

7 | CONCLUSIONS

Photovoltaic plant PMMA covering boxes frequently break. Understanding the reason for this fracture is the study's key goal. The main contribution of this work is the identification of "styrene" as the primary cause of fracture. Outside tests allowed replicating the door breaking. The article provides precise recommendations for selecting a door material that will minimize the occurrence of "crazing" problems. The performance of photovoltaic modules is not a topic covered by this investigation.

The PMMA "glass" of the fiberglass boxes may become brittle and break under various loads. The incompatibility between PMMA and SMC rises with the increase of styrene content, due to the relatively low copolymerization during the molding step in the synthesis of SMC. This is further supported by the fact that styrene makes PMMA plastic. The following phenomena have been also studied: hot properties, accidental bumps, thermal stresses, aging of the materials, outdoor aging, and cyclic loads. Thanks to the theoretical analysis, it is possible to verify that the PMMA can be easily broken.

All the potential causes of breakage need to be evaluated with attention. The fiberglass boxes can be installed in different environments; the wind, temperature, and humidity are specific for each solar plant. The boxes can vibrate in a different way depending on how they are secured. Each PMMA plate can present different defects according to the production process.

The physical experiments performed support the theory. The door is broken during the outdoor aging and not during the cycle test in the climatic chamber; this delayed effect is typical of the crazing, and low temperatures have accelerated the phenomena.

The study presented in this paper has one scientific objective and one industrial objective. The scientific objective is to understand how PMMA "glass" doors react to environmental stress-crazing events. The industrial objective is to choose the best "glass" for the door, based on the application.

This environmental crazing investigation pushes us to examine polymer "glass" thermoplastic blends further. Selecting a polymer matrix material that is more compatible with SMC support may be advisable. According to preliminary findings, PC is far more resistant to this crazing effect than PMMA. Replacing PMMA with PC has eliminated the problem of cracks in this application.

AUTHOR CONTRIBUTIONS

Francesco Cepolina: Investigation (lead). **Serena Gabrielli:** Formal analysis (lead). **Guido Ferla:** Methodology (lead). **Enrico Marcantoni:** Validation (lead). **Lorenzo Spinelli:** Data curation (lead).

ACKNOWLEDGMENT

Open Access Funding provided by Universita degli Studi di Genova within the CRUI-CARE Agreement.

DATA AVAILABILITY STATEMENT

Research data are not shared.

ORCID

Francesco Cepolina https://orcid.org/0000-0003-1481-4120

REFERENCES

[1] R. Rudolf, D. Popović, S. Tomić, R. Bobovnik, V. Lazić, P. Majerič, et al., *Materials* **2020**, *13*, 2717.
[2] V. Shah, *Handbook of Plastics Testing and Failure Analysis*, John Wiley & Sons, California **2020**.
[3] D. P. Tabor, L. M. Roch, S. K. Saikin, C. Kreisbeck, D. Sheberla, J. H. Montoya, et al., *Nat. Rev. Mater.* **2018**, *3*, 5.
[4] X. X. Zheng, A. J. Böttger, K. Jansen, J. van Turnhout, J. van Kranendonk, *Front. Mater.* **2020**, *7*, 437.
[5] R. P. Kambour, *J.Polym. Sci. Macromol. Rev.* **1973**, *7*, 1.
[6] L. Zhou, Y. Wang, Q. Huang, *Renew. Energy* **2019**, *138*, 754.
[7] A. M. Donald, E. J. Kramer, *Philos. Mag. A* **1981**, *43*, 857.
[8] C. Yiheng, *Acta Mech. Sin.* **2002**, *18*, 429.
[9] J. F. Fellers, D. C. Huang, *J. Appl. Polym. Sci.* **1979**, *23*, 2315.
[10] C. C. Hsiao, J. A. Sauer, *J. Appl. Phys.* **1950**, *21*, 1071.
[11] C. A. Harper, *Handbook of Plastic Processes*, John Wiley & Sons, New Jersey **2006**, p. 1.
[12] H. Lee, M. Huh, J. Yoon, D. Lee, S. Kim, S. Kang, *Carbon Lett.* **2017**, *22*, 101.
[13] R. Molfino, M. Zoppi, F. Cepolina, J. Yousef, E. E. Cepolina, *WSEAS Trans. Circuits Syst.* **2014**, *13*, 253.
[14] M. Nuruddin. Molecular Transportation in Polymer and Composite Materials: Barrier Performance and Mechanical Property Evaluation Doctoral Dissertation Purdue University. **2020**.
[15] S. Veerasingam, M. Ranjani, R. Venkatachalapathy, A. Bagaev, V. Mukhanov, D. Litvinyuk, et al., *Crit. Rev. Environ. Sci. Technol.* **2021**, *51*, 2681.
[16] R. Huszank, E. Szilágyi, Z. Szoboszlai, Z. Szikszai, *Nucl. Instrum. Methods Phy. Res. B* **2019**, *450*, 364.
[17] J. H. Butler, D. C. Joy, G. F. Bradley, S. J. Krause, *Polymer* **1995**, *36*, 1781.
[18] T. Cunningham, F. M. Serry, L. M. Ge, D. Gotthard, D. J. Dawson, *Surf. Eng.* **2000**, *16*, 295.
[19] J. Z. Kovacs, K. Andresen, J. R. Pauls, C. P. Garcia, M. Schossig, K. Schulte, W. Bauhofer, *Carbon* **2007**, *45*, 1279.
[20] V. V. Moshev, S. E. Evlampieva, *Polym. Eng. Sci.* **1997**, *37*, 1348.
[21] I. S. Kim, H. Cho, K. S. Sohn, K. Kim, S. Kim, *Eng. Fail. Anal.* **2021**, *129*, 105719.
[22] M. N. Sarrion, F. J. Santos, M. T. Galceran, *J. Chromatogr. A* **1999**, *859*, 159.
[23] Q. L. Ma, N. Hamid, A. E. D. Bekhit, J. Robertson, T. F. Law, *Microchem. J.* **2013**, *111*, 16.
[24] J. S. Elmore, D. S. Mottram, E. Hierro, *J. Chromatogr. A* **2001**, *905*, 233.
[25] C. W. Ho, W. M. Wan Aida, M. Y. Maskat, H. Osman, *J Food Compos. Anal.* **2006**, *19*, 822.
[26] B. Zorc, M. Zorc, B. Kosec, A. Nagode, *Polymer* **2020**, *12*, 280.

[27] J. A. Jensen, *Environmental stress cracking "The Plastic Killer"*, Adv Mater Processes, Ohio, USA **2004**, p. 50.
[28] T. S. Carswell, H. K. Nason, *Mod. Plast.* **1944**, *21*, 121.
[29] A. A. Abdel-Wahab, S. Ataya, V. V. Silberschmidt, *Polym. Test.* **2017**, *58*, 86.
[30] PLAZIT POLYGAL. PLAZCRYL SUPER Extruded high impact polymethyl methacrylate. **2023** Retrieved from: https://plazit-polygal.com/wp-content/uploads/2021/03/PLAZCRYL-SUPER-Extruded-high-impact-Polymethyl-Methacrylate-PMMA-solid-sheets.pdf.
[31] J. Wang, L. F. Peng, Y. J. Deng, X. M. Lai, M. W. Fu, J. Ni, *Int. J. Plast.* **2019**, *122*, 135.
[32] F. E. Cepolina, G. G. Muscolo, *ISR/Robotik 2014; 41st International Symposium on Robotics*, VDE, Munich, Germany **2014**, p. 1.
[33] P. Matteucci, F. Cepolina, *Autom. Constr.* **2015**, *58*, 109.
[34] H. H. Kausch, G. H. Michler, *The Effect of Time on Crazing and Fracture*, Vol. I, Springer, Berlin, Heidelberg **2005**, p. 1.
[35] W. Macek, R. Branco, M. Szala, Z. Marciniak, R. Ulewicz, N. Sczygiol, P. Kardasz, *Materials* **2020**, *13*, 3691.
[36] W. Liu, X. Yao, X. Chen, *Int. J. Fatigue* **2017**, *103*, 436.
[37] E. M. Cepolina, F. Cepolina. Twin Tools for Intelligent Manufacturing: A Case Study. In Proceedings of the 23rd International Conference on Harbor, Maritime and Multimodal Logistic Modeling and Simulation. **2021**.
[38] F. Cepolina, E. M. Cepolina, *Robotics in Natural Settings: CLAWAR*, Springer International Publishing, Cham **2022**, p. 501.
[39] F. Cepolina, E. M. Cepolina, *Int. J. Simul. Process Model.* **2022**, *18*, 329.

How to cite this article: F. Cepolina, S. Gabrielli, G. Ferla, E. Marcantoni, L. Spinelli, *J. Appl. Polym. Sci.* **2023**, e53961. https://doi.org/10.1002/app.53961